

Numerical Investigation on the Effect of Steel Strip Feeding on Solidification in Continuous Casting

Ran Niu, Baokuan Li, Zhongqiu Liu and Xianglong Li

Abstract Steel strip feeding into continuous casting mold is an innovative technology improving the thick slab quality through decreasing the melt superheat and increasing the proportion of equiaxed dendrites. To investigate the embedded complex melting and solidification processes, a mathematical model has been developed to model all the essential physical behaviors of the fluid flow, heat transfer, melting and solidification during steel strip feeding into the mold. The enthalpy method is adopted to describe both the melting of steel strip and the solidification of slab. Based on the numerical findings, three periods are divided during the whole melting process of the moving strip. The effect of strip feeding on the fluid flow, temperature distribution and shell solidification in continuous casting mold are investigated. The turbulent flow in the mold is enhanced due to the fast moving of strip and the fluid nearby is cooled down which redistributes the melt superheat inside slab.

Keywords Melting · Strip feeding · Continuous casting · Heat transfer

Introduction

Recently developments of continuous casting (CC) technology have resulted in a great increase of production capacity of cast bloom. Eliminating or significantly reducing the defects is of great importance to achieve satisfactory products [1]. A creative method that adding vibrating consumable strip to mold has been put forward by the Azovstal' Metallurgical Combine in Ukraine, to alleviate segregation and central porosity defects of CC slab [2, 3]. The concept of the process can be illustrated in a schematic diagram as shown in Fig. 1.

As depicted, a thin consumable steel strip is fed into the liquid metal in the mold by a strip feeding apparatus. The strip feeding apparatus is mainly consists of a few

R. Niu · B. Li (✉) · Z. Liu · X. Li
School of Metallurgy, Northeastern University, Shenyang 110819, Liaoning, China
e-mail: libk@smm.neu.edu.cn

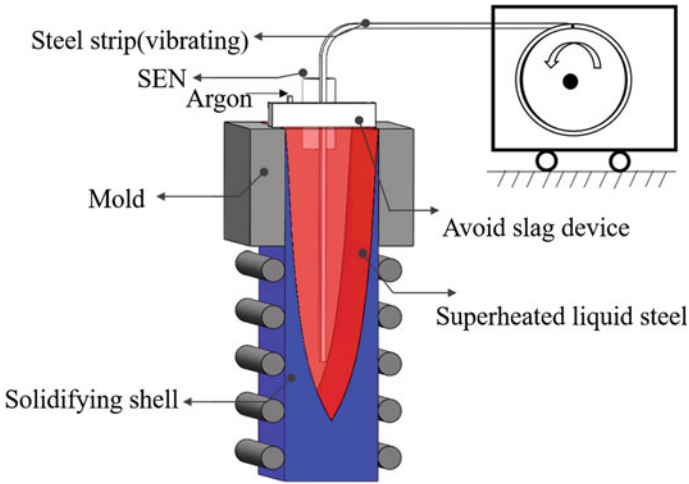


Fig. 1 Schematic diagram of the strip feeding process

main units for strip storage, strip sending and strip straightening. Chemical composition of the strip must be chosen to match with the composition of the slab. The strip is fed at the speed much faster than the casting speed to vicinity of the SEN for removing the superheat directly from the central part of the slab. At the same time, for preventing the entrapment of mold flux, an argon protection is equipped around the strip at the top surface. Benefit from the melting of strip, the superheat at the central of a slab could be decreased. The nucleation formation could be therefore promoted; widening the equiaxed zone and narrowing the columnar dendritic zone. Furthermore, the strip also accelerates the slab solidification rate; increasing the casting speed and the corresponding continuous caster capacity. The above advantages may make the strip feeding technology becoming an economical alternative to improve the quality of slab in compared to other expensive and complex technologies [3].

The present work undertakes to investigate the characteristics of steel strip melting in a liquid steel flowing continuous casting mold. A coupled model including fluid flow, heat transfer and phase change is developed to describe the strip melting and the strand shell solidifying, simultaneously. The strip melting evolution, melting rate and its effect on the distribution of turbulence and temperature in mold are studied

Mathematical Model

In order to investigate the phase change of the moving strip inside the continuous casting mold, a three-dimensional numerical model which incorporates all the essential physical phenomena such as fluid flow, heat transfer, solidification and

melting has been proposed and developed. To simplify the calculation, in the present study, the strip feeding technology is applied to a round bloom. The cast bloom is considered as perfectly vertical and the solid steel strip is assumed to be fed vertically throughout the whole melting process. As a straight nozzle is adopted, the jet flow has little influence on the movement of the strip, so only the movement along the feeding direction is taken into considered. The strip with the same properties as the melt, the convective effect of solutes is neglected.

General Equations of the Model

The continuity and momentum equations under turbulent conditions are:

$$\frac{\partial(\rho u_i)}{\partial x_i} = 0 \quad (1)$$

$$\rho \frac{\partial u_i u_j}{\partial x_j} = \frac{\partial}{\partial x_j} \left[\mu_{eff} \left(\frac{\partial u_i}{\partial x_j} + \frac{\partial u_j}{\partial x_i} \right) \right] - \frac{\partial P}{\partial x_i} + \rho g_i + F_B + S_p \quad (2)$$

where μ_{eff} , the effective viscosity coefficient, is the sum of the laminar (μ_l) and turbulent (μ_t) viscosity.

To calculate turbulence viscosity and phase change phenomena simultaneously in the continuous casting process, the low-Reynolds number k- ϵ eddy viscosity model is applied. The turbulent viscosity formulation as a function of turbulent kinetic energy, k, and dissipation rate of turbulent kinetic energy, ϵ , is defined as:

$$\mu_t = \rho \cdot C_\mu \cdot \frac{k^2}{\epsilon} \quad (3)$$

where C_μ is a function of the mean strain and rotation of the fluid, and it prevents unrealizable values for the large mean strain rate. The model coefficients used in this study is based on the empirical constants, $C_\mu = 0.09$ [4].

A sink term S_p is presented in the momentum equation to account for the resistance force induced by columnar dendrites and is described with the Darcy's Law:

$$S_p = \frac{(1 - \beta^2)}{(\beta^3 + \epsilon)} A_{mush} (u_i - u_{s,i}) \quad (4)$$

where $(u_i - u_{s,i})$ is the relative motion between fluid phase and solid phase, $u_{s,i}$ is the average solid phase velocity in direction i ; In slab shell pulling zone, $u_{s,i} = v_c$; In strip feeding zone, $u_{s,i} = v_a$. v_c and v_a are casting-speed and feeding strip speed, respectively. ϵ is a small number (0.001) to avoid dividing by zero; A_{mush} is the mushy zone constant to describe the attenuation level of velocity.

For the source term in Eq. (2), F_B is the thermal buoyancy due to the non-isothermal flow field induced by strip melting and slab cooling boundary conditions. The thermal buoyancy effect in momentum equations is assumed with the Boussinesq approximation, the gravity source term-natural convection is defined as follows:

$$F_B = \frac{\rho\beta_T(H-H_{ref})}{c_l} g_i \quad (5)$$

where c_l is the liquid steel specific heat, H_{ref} is the enthalpy of the reference temperature.

The general equation for melting, solidification and heat transfer is:

$$\frac{\partial(\rho H)}{\partial t} + \frac{\partial(\rho u_j H)}{\partial x_j} = \frac{\partial}{\partial x_j} \left[\left(\lambda_{eff} + C_p \frac{\mu_t}{\sigma_t} \right) \frac{\partial H}{\partial x_j} \right] \quad (6)$$

where H is the enthalpy and λ_{eff} is the thermal conductivity coefficient [5]. σ_t is the turbulent Prandtl number, and equals to 1.0.

The temperature-dependent conductivity is given as follows [6]:

$$\lambda_{eff}(T) = \begin{cases} \lambda_s = 13.86 + 1.113T \times 10^{-2} & T < T_s \\ \lambda_s + \frac{\lambda_l - \lambda_s}{T_l - T_s} (T - T_s) & T_s \leq T \leq T_l \\ \lambda_l = 39 & T > T_l \end{cases} \quad (7)$$

The enthalpy H over a temperature range is described by the following equations:

$$H(T) = \begin{cases} c_s T & T < T_s \\ c_s T + \frac{L(T-T_s)}{(T_l-T_s)} & T_s \leq T \leq T_l \\ c_s T + L + c(T_l - T_s) & T > T_l \end{cases} \quad (8)$$

Boundary Conditions

The heat transfer and solidification problem of the 500 mm bloom is complicated by the varying cooling boundary conditions along the casting direction. The detailed boundary conditions of heat transfer at the bloom surface are summarized as follows:

- (1) The heat loss along the casting direction firstly occurs in cooper mold cooled by water, the flux of heat transferred is given as [7]:

$$q = \frac{\rho c_w W (T_{in} - T_{out})}{S} \quad (9)$$

where W is cooling water flux, $\text{m}^3 \text{h}^{-1}$, T_{in} and T_{out} are the cooling water temperature in and out of mold, S is the contact area between melt and mold, m^2 .

- (2) Following the cooper mold is the secondary cooling zone where cooling water sprayed on the freezing shell surface directly by nozzle, surface heat transfer coefficient is:

$$h_{spray} = A \times Q_w^c \times (1 - b \times T_{spray}) \quad (10)$$

where Q_w^c is water flux in the spray zones. According to the Nozaki's empirical correlation, $A = 0.3025$ and $b = 0.0075$, which has been used successfully by other modellers [8].

- (3) Below the secondary cooling section is the radiation zone, where the heat is removed by the radiation and convection to the surrounding air. In radiation zone, the heat extraction due to radiation can be evaluated as [9]:

$$h_{rad} = \sigma \times \varepsilon (T_{surf} + T_{amb}) (T_{surf}^2 + T_{amb}^2) \quad (11)$$

Computational Procedure

To ensure the accuracy and efficiency of the coupled model, the computational domain of the continuous casting system is reasonably divided according to the characteristic of macroscopic transport during casting process. It is observed that the melt in a small distance below the meniscus shows a turbulent flow pattern. And then the plug flow is formed when the fluid velocity equals to casting speed. So the whole computational domain is divided into two main regions: turbulent flow region and laminar flow region. To transmit the datum like velocity, temperature and liquid fraction between the two regions, the coordinate interpolation algorithm is adopted. A schematic diagram of the computational domain, cooling boundary conditions and the meshes of the two regions are illustrated in Fig. 2. A velocity-inlet boundary condition was imposed at the top SEN. The melt inlet velocity and the strip inlet was specified according to the casting and feeding speed respectively. Initially, the solid phase strip was assumed to be at ambient temperature of $20 \text{ }^\circ\text{C}$ and the liquid steel is specified at a superheat temperature of 10, 30 and 50 K respectively. All the governing equations were discretized by the finite volume method (FVM). The SIMPLE algorithm was adopted to resolve the velocity-pressure coupling in the momentum equation. Moreover, the upwind differencing scheme was used to approximate the convective and diffusive terms giving second order accuracy in space and time. Throughout the simulation, the liquid fraction was updated based on the temperature from the previous time step by solving the discretized equations associated with the appropriate boundary conditions. For melting, the volume temperature at the previous time-step should be

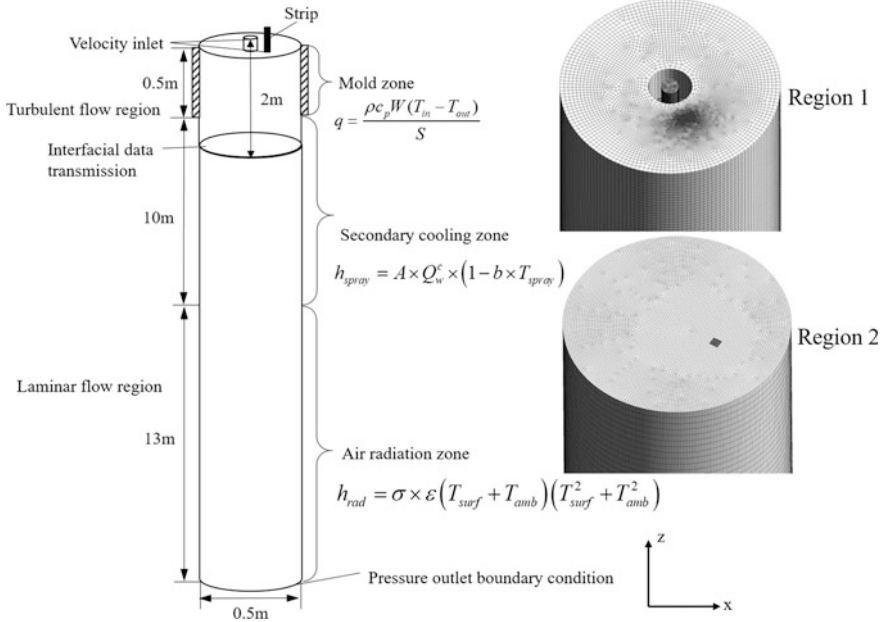


Fig. 2 Schematic diagram of the computational domain, cooling boundary conditions and the meshed computational region division

lower than at the ‘actual’ time step, and vice versa for solidifying. This concept was therefore used to provide the solver with the required information to determine whether the steel in a specific volume is melting or solidifying. A fixed time step scale of 0.001 s was adopted for the entire simulation. The adopted thermophysical parameters for the steel and operating parameters are summarized in Table 1. The simulation was terminated until a pseudo-steady state has reached implying that the strip melting speed is roughly the same with the strip feeding speed and the strip tip is located in a fixed position with insignificant fluctuation.

Table 1 Thermophysical parameters for the steel and operating parameters in casting

Parameters	Value	Parameters	Value
Viscosity of the liquid steel (kg/m s)	6.2×10^{-3}	Casting speed (m/min)	0.35
Latent heat (KJ/kg)	272	Mold water inlet temperature (K)	298
Density (kg/m ³)	7020	Mold water outlet temperature (K)	306
Liquidus temperature (K)	1790	Mold cooling water flow rate (L/min)	4600
Solidus temperature (K)	1749	Secondary cooling water flow rate (L/min)	27

Results and Discussion

Validation

For melting, the accuracy of the mathematical model has been verified through comparison with experimental results performed in Baosteel [10]. Liquid steel is accommodated in a crucible which can be heated through the induction furnace. The strip is fed into the melt held by a strip holder controlled by a lifting device, as depicted in Fig. 3a. Here, the strip used was 3 mm thick. By lifting the strip out and measuring the thickness of strip at a 2 mm distance away from the tip at a fixed time interval, the total strip thickness evolution has been recorded. The comparison of the predicted and measured strip thickness versus immersion time is demonstrated in Fig. 3b. Reasonable agreement of the whole melting time as well as the maximum thickness of the strip was obtained indicating the reliability of the model.

Evolution of Strip Melting

Strip Thickness Evolution

According to the validation results, the process of melting with solidifying consists of three stages. During the first stage, a short period of sheath is formed in the immersed part of strip. The thickness of the sheath first increases and then reaches a maximum. After that, the sheath begins to melt until disappears. After melting of the sheath, melting of the strip starts. The third stage ends with complete melting of the strip, total melting time is t_m . A typical melting curve is presented in Fig. 4a to better understand mechanism of melting of strip in liquid metal. The complicated

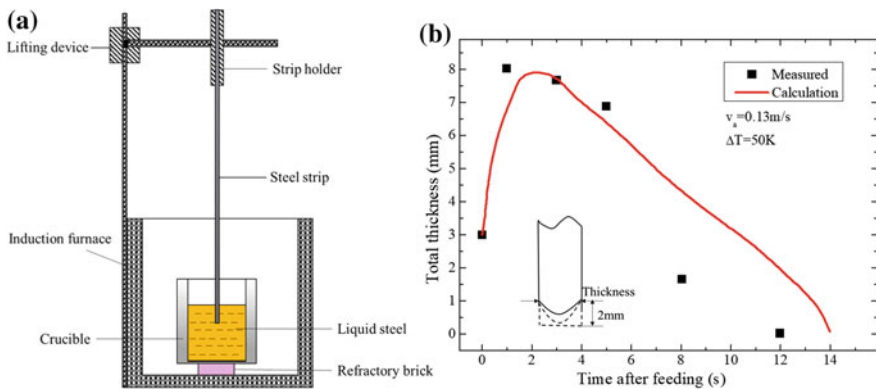


Fig. 3 a Schematic diagram of experiment b Comparison between experimental results and predicted results

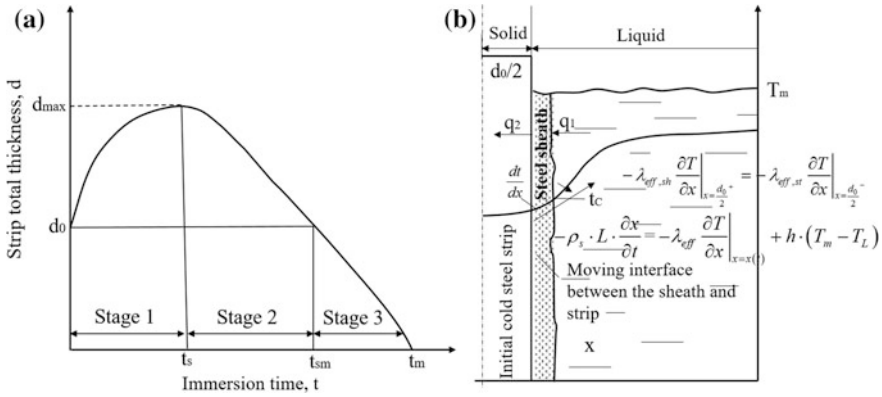


Fig. 4 a Melting curve of the strip versus time b The complicated heat transfer between the strip and liquid melt

heat transfer between the strip and the molten steel is depicted in Fig. 4b. At the first moment after immersion of the strip, due to high thermal conductivity of the strip, the magnitude of heat flux drawn by the strip is larger than the magnitude associated with the convective heat flux. During this period, the intensity of metal cooling by the strip is gradually reduced. The thickness of the sheath continues to increase, but the rate of this increase gradually drops. By the t_s , the strip temperature rises to such an extent that the intensity of liquid metal cooling becomes not high enough for the process of solidification of the sheath to continue. Then the further growth of the sheath thickness ceases. The melting of this solid sheath begins when the rate of heat transfer from the melt by convection becomes greater than the rate of heat conduction through the sheath. The end of the period II denotes the time at which the encasing steel sheath has entirely melted back to expose the original strip. The moving strip in the slab melt to vanish to avoid “the un-melted frozen in shell” before reaching the end of liquid core.

Strip Travels Distance

The distance travelled is the distance travelled by the strip before a dynamic steady state is got between the continuously poured in hot melt, cooling boundary conditions and the strip melting. The effect of strip feeding speed, strip initial thickness and liquid steel superheat on the distance travelled by the strip has been shown in Fig. 5. It has been observed that although the melting time decreases with the increase in strip feeding speed, whether the strip will travel deeper or not is dictated by whether the decrease in melting time is significantly higher or not. With the relatively low feeding speed, the distance travelled increases with strip feeding speed. With the increase of the strip thickness, the total heat requirement for melting of the strip increases as there is more strip mass to be melted and the strip travels

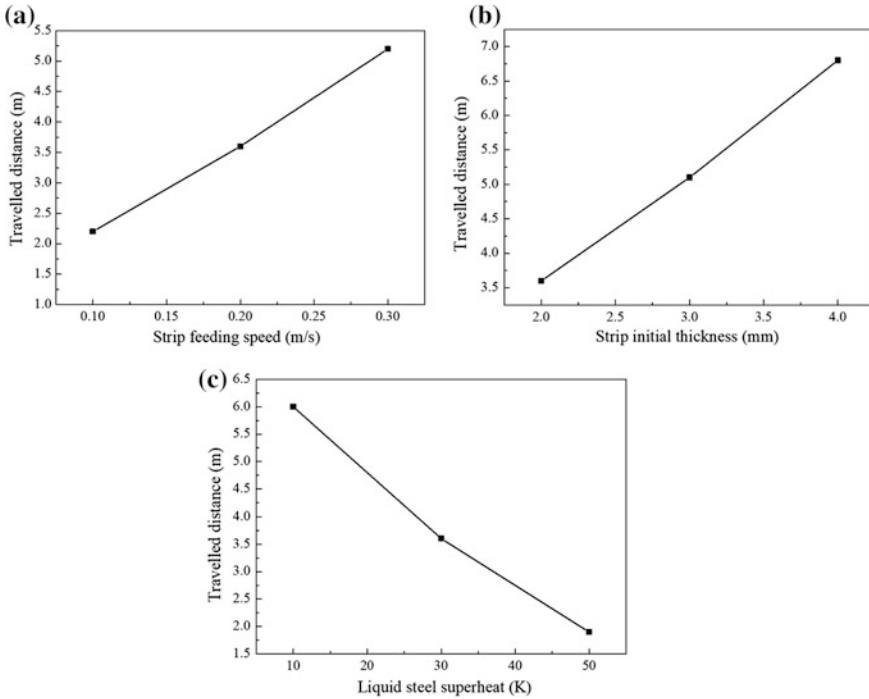


Fig. 5 The travelled distances of the strip under different feeding scenarios **a** Different strip feeding speeds **b** Different strip thicknesses **c** Different liquid steel superheat

longer. As the superheat is increased, the maximum thickness of the sheath decreases due to the increased amount of heat supplied from the melt to the strip. Additionally, the total melting time decreases and the travelled distance is decreased.

Effect of Strip Feeding on Fluid Flow

Figure 6 shows the three dimensional streamline distribution in mold with a strip feeding in, the strip morphology is also presented. The effect of the continuously moving strip on flow field can be clearly identified. It is seen that the molten steel, supplied by normal straight nozzle, passes straight down with a high speed and then tends upward approaching to the solidification shell. As the strip moves at a speed much faster than the flowing fluid (i.e., 0.2 m/s), the molten steel around it flows downward carried by the strip. Thus, the turbulent flow in the mold is enhanced. Meanwhile, with the cold strip melting, the nearby downward fluid is therefore cooled down. Outside the undercooled zone, the fluid is lighter and the buoyancy force is upward. This combination of the downward and upward fluids results in the enhancement of the recirculation of the fluid flow.

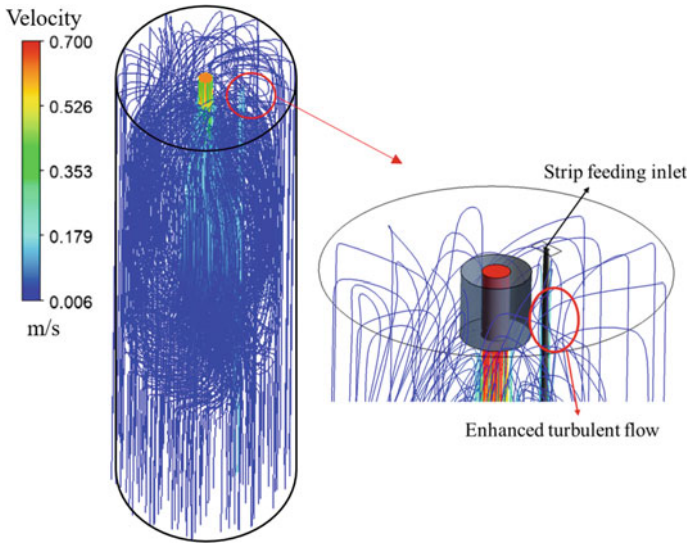


Fig. 6 The streamline distribution in a round bloom mold with a strip feeding in

Effect of Strip Feeding on Liquid Steel Superheat

Accompany with the phase change, the temperature of the melt around the strip is decreased. Figure 7 shows the temperature distribution around the strip during the three stages when a steady state is reached. It can also be observed that with the increment of the distance the strip travels, the strip temperature increases. Besides,

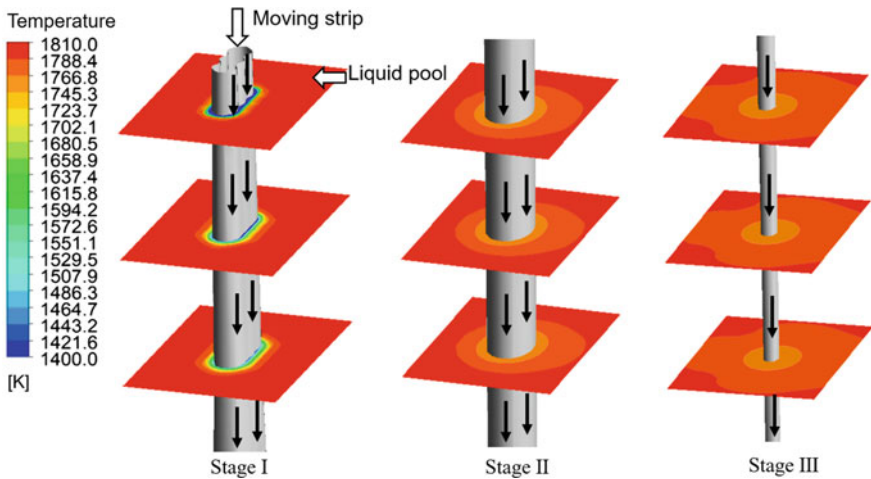


Fig. 7 Temperature distribution around the strip during the three stages

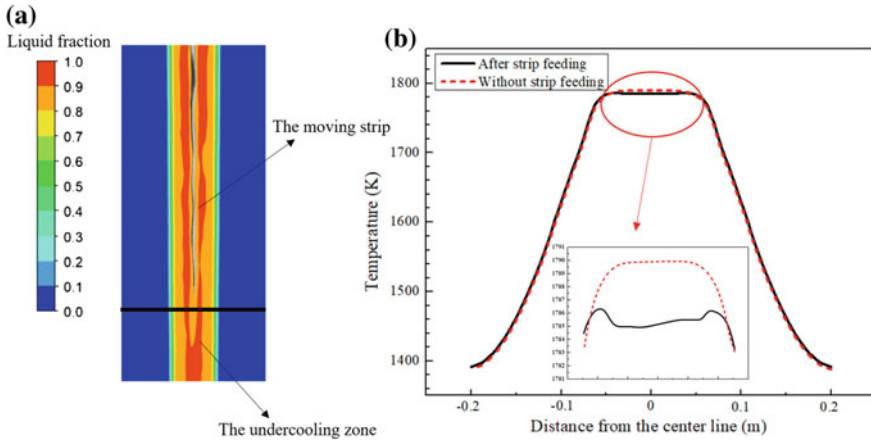


Fig. 8 Temperature decrease action by the end of liquid core

with the decreasing superheat of the liquid pool, the cooling effect is enhanced. On the other hand, it is seen that during the sheath formation stage I, the range of cooling zone is limited. As the melting goes on, the cooling zone range is further extended.

During the steady state, the strip tip is by the end of the slab liquid core, the strip and shell morphology are depicted in Fig. 8, and the temperature distribution along the black line is plotted. It is seen that after strip feeding, the temperature in the central zone is decreased by up to 5 K. And the range width of the action is around 0.1 m. Here, a strip with 3 mm thickness is adopted. The overcooled zone forms another center of solidification which is conducive to the development of equiaxed dendrites.

Conclusions

1. Steel strip suffers three periods when fed into the mold, including the steel sheath formation stage, steel sheath melting stage and steel strip melting stage.
2. The turbulent flow is enhanced by the forced convection induced by the fast moving strip. And due to the cooling effect of the strip, the combination of the downward and upward fluids enhances the recirculation of the fluid flow.
3. The melt superheat in the vicinity of the strip is decreased by up to 5 K at melting end. And a 0.1 m overcooled zone is developed around the moving strip to form another center of solidification.

Acknowledgements This work was financially supported by the National Natural Science Foundation of China (No: 51574068) and the Fundamental Research Funds for the Central Universities (No. N162504009).

References

1. Luo S et al (2014) Characteristics of solidification structure of wide-thick slab of steel Q345. In: 5th International Symposium on High-Temperature Metallurgical Processing. TMS, Warrendale
2. Isaev OB (2005) Effectiveness of using large cooling elements to alleviate axial segregation in continuous-cast ingots. *Metallurgist* 49(7):324–331
3. Golenkov MA (2014) Improvement of internal quality of continuously cast slabs by introducing consumable vibrating macrocoolers in a mold. *Russ Metall* 12:961–965
4. Sun H, Zhang J (2014) Study on the macrosegregation behavior for the bloom continuous casting: model development and validation. *Metall Mater Trans B* 45(3):1133–1149
5. Hu H, Argyropoulos SA (1996) Mathematical modelling of solidification and melting: a review. *Modell Simul Mater Sci Eng* 4(4):371–396
6. Li C, Thomas BG (2004) Thermomechanical finite-element model of shell behavior in continuous casting of steel. *Metall Mater Trans B* 35(6):1151–1172
7. Alizadeh M, Jenabali JA, Abouali O (2008) A new semi-analytical model for prediction of the strand surface temperature in the continuous casting of steel in the mold region. *Isij Int* 48(2):161–169
8. Hardin RA, Liu K, Beckermann C, Atul K (2003) A transient simulation and dynamic spray cooling control model for continuous steel casting. *Metall Mater Trans B* 34(3):297–306
9. Melissari B, Argyropoulos SA (2005) Development of a heat transfer dimensionless correlation for spheres immersed in a wide range of Prandtl number fluids. *Int J Heat Mass Trans* 48(21):4333–4341
10. Li YT, Zhang L, Zhang HW (2011) Melting process of steel strip and microstructure of ingot with steel-strip fed in molten steel. *J Iron Steel Res* 23(11):54–58